

Accurate Descriptions of Hot Flow Behaviors Across β Transus of Ti-6Al-4V Alloy by Intelligence Algorithm GA-SVR

Li-yong Wang, Le Li, and Zhi-hua Zhang

(Submitted May 5, 2016; in revised form June 4, 2016; published online July 18, 2016)

Hot compression tests of Ti-6Al-4V alloy in a wide temperature range of 1023–1323 K and strain rate range of $0.01\text{--}10\text{ s}^{-1}$ were conducted by a servo-hydraulic and computer-controlled Gleeble-3500 machine. In order to accurately and effectively characterize the highly nonlinear flow behaviors, support vector regression (SVR) which is a machine learning method was combined with genetic algorithm (GA) for characterizing the flow behaviors, namely, the GA-SVR. The prominent character of GA-SVR is that it with identical training parameters will keep training accuracy and prediction accuracy at a stable level in different attempts for a certain dataset. The learning abilities, generalization abilities, and modeling efficiencies of the mathematical regression model, ANN, and GA-SVR for Ti-6Al-4V alloy were detailedly compared. Comparison results show that the learning ability of the GA-SVR is stronger than the mathematical regression model. The generalization abilities and modeling efficiencies of these models were shown as follows in ascending order: the mathematical regression model < ANN < GA-SVR. The stress-strain data outside experimental conditions were predicted by the well-trained GA-SVR, which improved simulation accuracy of the load-stroke curve and can further improve the related research fields where stress-strain data play important roles, such as speculating work hardening and dynamic recovery, characterizing dynamic recrystallization evolution, and improving processing maps.

Keywords constitutive model, flow stress, genetic algorithm, support vector regression, titanium alloy

1. Introduction

Ti-6Al-4V alloy, a typical $\alpha + \beta$ titanium alloy, has the advantages of high strength, low density, excellent stress-corrosion resistance etc., so it was widely used in aerospace industry. It is widely acknowledged that stress-strain data play important roles in many areas, for examples, speculating work hardening (WH) and dynamic recovery (DRV) (Ref 1), improving processing maps (Ref 2), characterizing dynamic recrystallization (DRX) evolution (Ref 3), etc. A prediction model which can accurately track flow behaviors and predict stress-strain data is critical to reflect material properties and further improve the related research fields where stresses play important roles. Thereby, it is important to construct a model to accurately characterize the highly nonlinear flow behaviors of Ti-6Al-4V alloy.

So far, there exist three typical models in characterizing flow behaviors of metals, namely, empirical/semiempirical model, analytical model, and phenomenological model (Ref 4–6). The analytical model requires systematic and detailed investigation

of microscopic deformation mechanisms such as dislocation theory, static coarsening, and dynamic coarsening (Ref 7). Voyiadjis and Abed constructed the analytical constitutive models involving dislocations interaction mechanisms for the flow behaviors of face-centered cubic (FCC) and body-centered cubic (BCC) metals at different strain rates and temperatures (Ref 8). In the study of Voyiadjis and Abed, the mobile dislocation density has different impacts on flow behaviors at different temperatures and strain rates, so it needs to build different analytical constitutive models at different deformation conditions; otherwise, the analytical constitutive models cannot precisely track the highly nonlinear deformation behaviors (Ref 8). In addition, analytical constitutive models need a lot of precise experiment data to construct mathematical models of complicated microscopic deformation mechanisms. Thereby, analytical models have not been extensively adopted for characterizing flow behaviors of metals.

Phenomenological model includes mathematical regression equation and intelligence algorithm, and it does not require systematic and detailed investigation of microscopic deformation mechanisms. At present, the typical Arrhenius-type equation of phenomenological model, and its improved forms were used to characterize flow behaviors of many materials, such as pure titanium (Ref 9) and Ti-6Al-4V (Ref 10). Other mathematical regression equations of phenomenological model involve the representative Khan-Huang-Liang (KHL) model and Johnson-Cook (JC) model. Mathematical regression equations only need to calculate some necessary material constants and further fit experimental data, so they have been widely used. However, mathematical regression equations have large fluctuant accuracies at different strain rates and temperatures (Ref 11–14). Because the mathematical regression equations which are mathematically fitted according to limited experi-

L. Wang, Collaborative Innovation Center of Electric Vehicles in Beijing, Beijing Information Science and Technology University, Beijing 100192, China; and **Le Li** and **Zhi-hua Zhang**, The Ministry of Education Key Laboratory of Modern Measurement and Control Technology, Beijing Information Science and Technology University, Beijing 100192, China. Contact e-mail: wangliyong2004@163.com.

mental data cannot accurately track the highly nonlinear flow behaviors at different strain rates and temperatures (Ref 13, 15).

Recently, artificial neural network (ANN) of intelligence algorithm which imitates biological neural systems was utilized to characterize the flow behaviors of many metals, such as 42CrMo steel (Ref 16), as-cast Ti60 titanium alloy (Ref 17), and as-cast TC21 (Ref 18). ANN needs to try a lot of network topologies and training parameters to acquire a higher accuracy level, which will consume much time and energy. For a certain dataset, the same network topology and training parameters of an ANN will obtain fluctuant accuracies in different attempts. ANN can encounter well network topology and training parameters to reach a higher accuracy level; however, this accurate results have poor reproducibility. Besides, ANN is easy to fall into local extremum and cannot obtain a globally optimal solution.

Support vector regression (SVR) is a machine learning method based on statistical learning theory and structural risk minimization principle, which is generally utilized in regression analysis area (Ref 19). SVR has the merits of strong generalization ability and robustness. Compared with ANN, SVR can avoid falling into local extremum and obtain a globally optimal solution. For a certain dataset, a SVR with same training parameters will keep training accuracy and prediction accuracy at a stable level in different attempts. In this work, SVR was adopted for characterizing the hot flow behaviors of Ti-6Al-4V alloy on account of its excellent advantages. The learning ability and generalization ability of a SVR depend on the three parameters (penalty factor C , kernel parameter γ , and insensitive loss function ζ), especially the mutual influences among them. A SVR with suitable parameters C , γ , and ζ will accurately study the hot flow behaviors of Ti-6Al-4V alloy and appropriately ignore some singular points of stress-strain data. The impacts of the three parameters (C , γ , and ζ) on the learning ability and generalization ability of SVR should be comprehensively considered. It is inefficient to manually adjust the three parameters one by one to construct an accurate SVR in characterizing the hot flow behaviors of Ti-6Al-4V alloy. Thereby, it is crucial to find a stable and efficient way to realize the optimal selection of the three parameters (C , γ , and ζ) in SVR.

Lou et al. developed a SVR combined with particle swarm optimization (PSO) for characterizing the flow behaviors of AZ80 magnesium alloy. In the model, PSO was adopted to select the parameters C , γ , and ζ . This work indicated that the model is more precise than ANN and mathematical regression equations, meanwhile the sample dependence of the SVR is lower (Ref 20). Desu et al. established a SVR for characterizing the flow behaviors of Austenitic Stainless Steel 304, and the research of them indicated that SVR is more accurate, efficient, and reliable than the mathematical regression equations such as Johnson-Cook model, revised-Zerilli-Armstrong model, revised-Arrhenius model, and intelligence algorithm ANN (Ref 21). The best correlation coefficient (R) in their work is 0.9989 at a high accuracy level; however, they just attempted few parameter combinations of the three parameters (C , γ , and ζ), and there is still room for improvement in accuracy and efficiency (Ref 21).

GA, as a bionic and global optimization algorithm, was extensively used in multiparameters optimization problem on account of its advantages of strong robustness, high efficiency, and parallel processing. GA searches the global optimum in solution space by imitating the natural selection process and genetic mechanism (Ref 22). In this work, in order to utilize the

advantages of GA, it was combined with SVR to construct the flow stress prediction model of Ti-6Al-4V alloy where GA was used to efficiently search the optimal parameter combination of the three parameters (C , γ , and ζ), and the model was called as GA-SVR in this study. Compared with the work of Desu et al. (Ref 21), the GA-SVR can self-adaptively and dynamically search the optimal parameter combination of the three parameters (C , γ , and ζ) to obtain the most accurate prediction model for Ti-6Al-4V alloy, which greatly enhances the accuracy.

Subsequently, the learning abilities, generalization abilities, and modeling efficiencies of the mathematical regression model, ANN, and GA-SVR were compared. A standard statistical parameter, average absolute relative error ($AARE$), was adopted to assess the prediction performance of these models. In the comparisons of study abilities, the GA-SVR has larger R values and lower $AARE$ values, which show the GA-SVR can sufficiently learn the training samples and the study ability of the GA-SVR is stronger than the mathematical regression model. In the comparisons of generalization abilities, GA-SVR has larger R values and lower $AARE$ values, which indicate that the GA-SVR can accurately predict the highly nonlinear flow behaviors. The generalization abilities of these models were displayed as follows in ascending order: the mathematical regression model < ANN < GA-SVR. The prominent character of GA-SVR is that it with identical training parameters will keep training accuracy and prediction accuracy at a stable level in different attempts for a certain dataset. GA-SVR only needs representative training samples from the investigation and then self-adaptively and automatically searches the three parameters C , γ , and ζ to obtain the most accurate model, which greatly enhances the computational efficiency. The time in modeling an accurate GA-SVR is shorter than ANN. The modeling efficiencies of these models were displayed as follows in ascending order: the mathematical regression model < ANN < GA-SVR.

In finite element software, if a software needs to invoke stress-strain data which are not beforehand inputted to the software, it commonly calculates unknown stress-strain data by mathematical interpolation means. However, hot flow behaviors of materials at different strain rates and temperatures are highly nonlinear. The mathematical interpolation way cannot correctly predict the stress-strain data of materials and will obtain incorrect simulation results. The stresses outside experimental conditions were predicted by the well-trained GA-SVR, which improves simulation accuracy of the load-stroke curve and can further improve the related research fields where stress-strain data play important roles.

2. Collection of Experimental Stress-Strain Data

The chemical compositions (wt.%) of the adopted Ti-6Al-4V alloy are as follows: Al-6.50, V-4.25, O-0.16, Fe-0.04, N-0.015, C-0.02, and H-0.0018, Ti (balance). The homogenized extruded metal bar of Ti-6Al-4V alloy was incised by wire-electrode cutting to 28 specimens with a height of 12 mm and diameter of 10 mm. Figure 1 shows the optical microstructure of the as-received Ti-6Al-4V alloy, in which β -phase distributes on the grain boundaries of α -phase. These 28 specimens were compressed on a servo-hydraulic and computer-controlled Gleeble-3500 machine. Graphite lubricants were applied to coat the contact surfaces of the anvils and test samples, so as to diminish

the friction and prevent bonding between them. The test samples were heated at a rate of 10 K/s and held at a certain temperature for 3 min to assure a uniform temperature and reduce material anisotropy. The 28 test samples were compressed with a height reduction 60% (true strain 0.9) at the strain rates of 0.01, 0.1, 1, and 10 s⁻¹, and the temperatures of 1023, 1073, 1123, 1173, 1223, 1273, and 1323 K. And then these compressed test samples were rapidly quenched into water to retain the microstructures acquired at high temperatures. Figure 2 shows

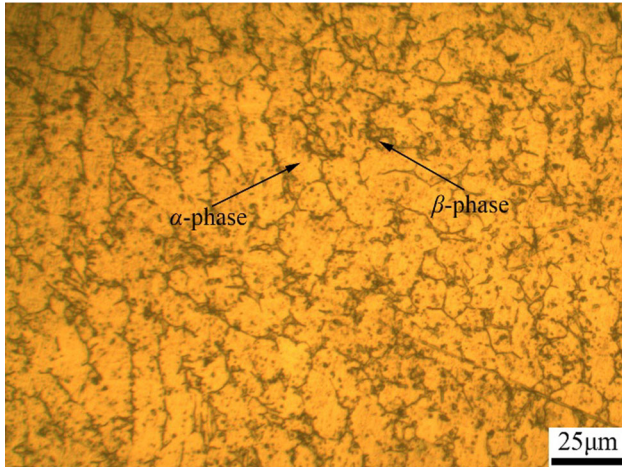


Fig. 1 Optical photograph of the as-received Ti-6Al-4V alloy

the experimental compressive stress-strain curves of Ti-6Al-4V alloy at different strain rates and temperatures. As shown in Fig. 2, it can be concluded that the flow stress level increases with the increase of strain rate for a certain temperature, and the flow stress level observably decreases with the increase of temperature for a certain strain rate. The flow stress evolution with strain can be briefly divided into three phases. At the first deformation phase, the flow stress quickly increases to a critical value with the increase of strain where WH dominates this phase; at the same time, the stored energy in grain boundaries increases quickly to the activation energy of DRX. At the second phase, DRX and DRV arise, and the increasing rate of flow stress decreases until a maximal stress where the thermal softening on account of DRX and DRV are balanced with WH. And the flow stress evolution involves two typical types at the third phase: the flow stress approximately keeps at a stable level which indicates a new dynamic balance between WH and DRV, such as the flow stress curves of 1223-1323 K and 0.01-0.1 s⁻¹; the flow stress continuously decreases with distinctly DRX softening, such as the flow stress curves of 1023-1173 K and 0.01 s⁻¹, 1023 K and 0.1 s⁻¹, and 1023-1173 K and 10 s⁻¹ (Ref 23). It is widely acknowledged that stress-strain data play important roles in many areas, for examples, speculating WH and DRV (Ref 1), improving processing maps (Ref 2), characterizing dynamic recrystallization evolution (Ref 3), etc. The existing literatures demonstrate that there are close relationships among temperature, strain, strain rate, and flow stress. A prediction model which can accurately track flow behaviors and further predict stress-strain data is critical to reflect material properties. Thereby, it is

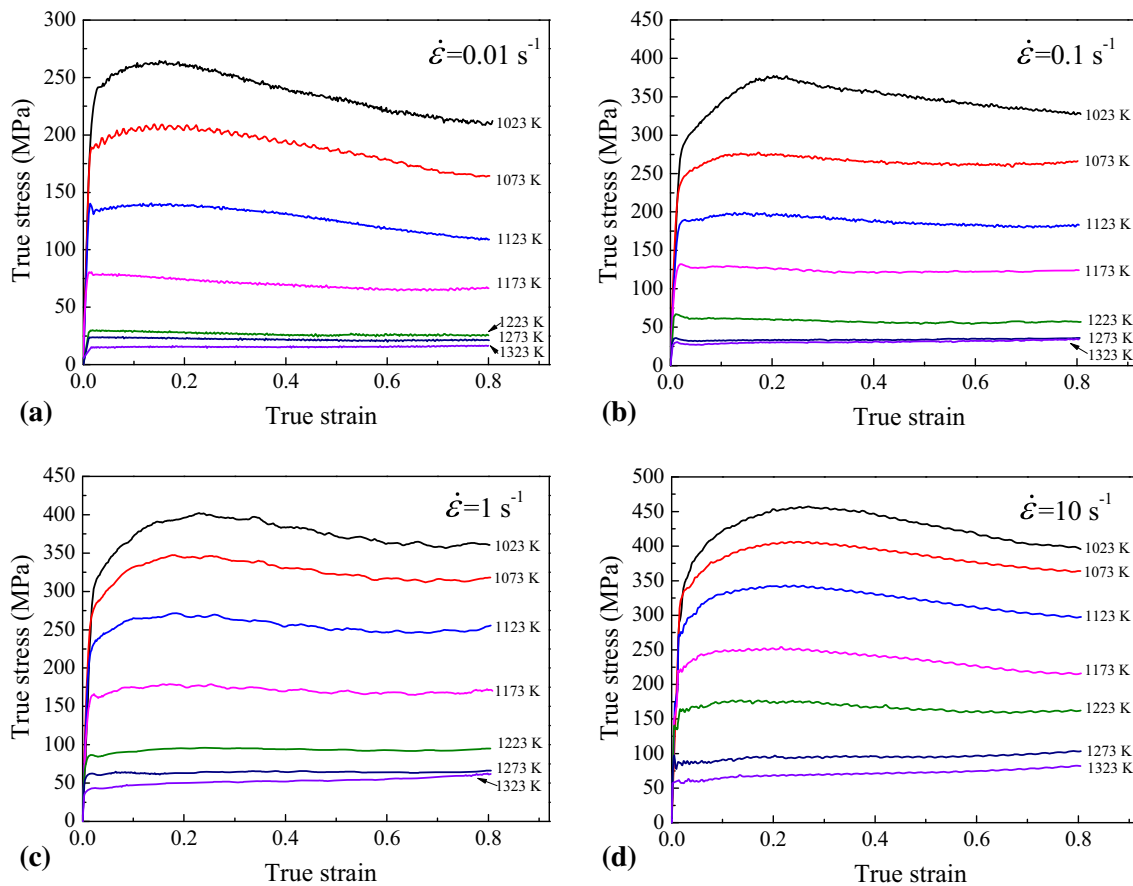


Fig. 2 True stress-strain curves of Ti-6Al-4V alloy at different strain rates and temperatures

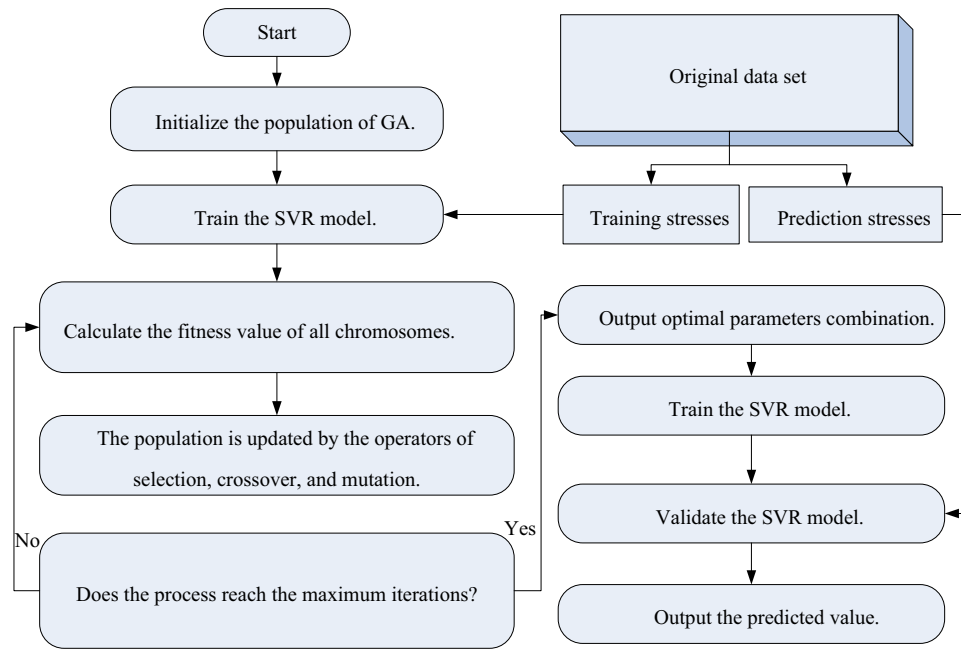


Fig. 3 The detailed flowchart of GA-SVR

important to construct a model to accurately characterize the highly nonlinear flow behaviors of Ti-6Al-4V alloy.

3. Development of Support Vector Regression (SVR) for the Flow Behaviors of Ti-6Al-4V Alloy

In this study, SVR was applied to establish the flow behaviors model of Ti-6Al-4V alloy on account of its excellent regression analysis ability and robustness.

3.1 The Basic Principles of SVR

SVR is a machine learning method based on statistical learning theory and structural risk minimization principle (Ref 19). The main merits of SVR are as follows. First, in SVR, the linearly inseparable low-dimensional data are mapped into linearly separable multidimensional data. Subsequently, SVR builds the linear discriminant function in high dimension space, and this method can conveniently handle the highly nonlinear data. Second, compared with ANN, the global optimum can be acquired using SVR. The computational process of SVR is robust and will avoid falling into local extremum.

In SVR, linearly inseparable low-dimensional data are mapped into linearly separable multidimensional data by kernel function $k(x_i, x_j) = \Phi(x_i) \cdot \Phi(x_j)$. And a SVR equipped with the radial basis function (RBF) of kernel function can reach a higher regression precision. Thereby, the RBF expressed as Eq 1 was applied to this work

$$k(x_i, x) = \exp(-\gamma \|x_i - x\|^2), \quad (\text{Eq 1})$$

where γ is variable parameter of the RBF.

In SVR, $y = f(x)$ can be expressed by Eq 2:

$$f(x) = \omega \cdot x + b, \quad (\text{Eq 2})$$

where ω is a multidimensional column vector and b is a bias term. It is assumed that original data are (x_1, y_1) , (x_2, y_2) , $(x_3,$

$y_3)$, ..., (x_i, y_i) , ..., (x_k, y_k) , $x_i, y_i \in \mathbb{R}$, and the function $f(x)$ is able to estimate all data. The optimal function can be expressed by:

$$\min \frac{1}{2} \|\omega\|^2 + C \sum_{i=1}^l (\xi_i + \xi_i^*), \quad (\text{Eq 3})$$

s.t.

$$\begin{cases} y_i - \omega \cdot x_i - b \leq \zeta + \xi_i \\ \omega \cdot x_i + b - y_i \leq \zeta + \xi_i^* \\ \xi_i, \xi_i^* \geq 0 \end{cases}, \quad (\text{Eq 4})$$

where ξ_i and ξ_i^* are slack variables which impact regression accuracy; C is the penalty factor; ω is a multidimensional column vector; and ζ is an insensitive loss parameter which greatly impacts regression accuracy of SVR. In this study, the input variables x of SVR are strain (ϵ), strain rate ($\dot{\epsilon}$) and temperature (T), and the output variable $f(x)$ is flow stress (σ) of Ti-6Al-4V alloy.

The regression function of optimal hyperplane in SVR is expressed by Eq 5:

$$f(x) = \sum_{i=1}^l (\alpha_i - \alpha_i^*) k(x_i, x) + b, \quad (\text{Eq 5})$$

where α_i is the Lagrange multiplier; $k(x_i, x)$ is a kernel function; and b is a bias term.

3.2 The Impact of Parameters Selection on the Performance of SVR

In SVR, the learning ability and generalization ability can be enhanced by suitable parameters settings, and these parameters are penalty factor C (expressed by Eq 3), the kernel parameter γ (expressed by Eq 1), and insensitive loss function ζ (expressed by Eq 4).

- (1) Penalty factor C : The robustness of SVR is influenced by the penalty factor C . In SVR, a larger C value indicates that all training samples should be accurately learned, which will cause the model to be complicated and over-fitting. Whereas a smaller C value in SVR indicates that some singular points can be neglected. In SVR, the phenomenon of under-fitting will appear when the penalty factor C value is too small.
- (2) The kernel parameter γ of RBF: As mentioned previously, the RBF expressed as Eq 1 was adopted in this work. The kernel parameter γ influences the generalization ability and learning ability of SVR. Severe over-fitting will appear in the following situations: (a) penalty factor C value is set as a certain numerical value and $\gamma \rightarrow \infty$; (b) C is set as a certain numerical value and $C \rightarrow \infty$ (Ref 24). And severe under-fitting will appear in the following situations: (a) C is set as a certain numerical value and $\gamma \rightarrow 0$; (b) C is set as a smaller numerical value and $\gamma \rightarrow \infty$; and (c) C is set as a certain numerical value and $C \rightarrow 0$ (Ref 24). An appropriate parameter γ can avoid over-fitting and under-fitting of data in SVR.
- (3) The insensitive loss function ζ : In SVR, the ζ value impacts the number of support vector and further influences the regression accuracy of the model.

It can be concluded that the learning ability and generalization ability of SVR depend on the three parameters C , γ , and ζ , especially the mutual influences among them. In SVR, in order to obtain an accurate model, it is time-consuming to manually optimize each parameter. The mutual effects of the three parameters (C , γ , and ζ) on learning ability and generalization ability of SVR should be comprehensively considered. It is inefficient to manually adjust the three parameters one by one to construct an accurate SVR in characterizing the hot flow behaviors of Ti-6Al-4V alloy. Thereby, it is crucial to find a stable and efficient way to realize the optimal selection of the three parameters in SVR. A SVR with suitable parameters C , γ , and ζ will accurately study the hot flow behaviors of Ti-6Al-4V alloy and appropriately ignore some singular points of stress-strain data.

3.3 The Stress Prediction Model Based on SVR and Genetic Algorithm (GA)

In this section, GA was combined with SVR to construct the flow stress prediction model of Ti-6Al-4V alloy where GA was utilized to efficiently search the optimal parameter combination of the three parameters (C , γ , and ζ), and the model was called as GA-SVR in this work.

3.3.1 The Basic Principles of GA. GA, as a bionic and global optimization algorithm, was extensively used in multi-parameters optimization problem on account of the advantages of strong robustness, high efficiency, and parallel processing. GA searches the global optimum in solution space by imitating the natural selection process and genetic mechanism (Ref 22). In GA, a population comprises a certain number of individuals which are encoded by gene encoding. After generation of initial population, optimal solutions are evolved in every generation.

The individuals are selected using a fitness function in every generation. Based on the fitness value of each individual, the individual which has a larger fitness value is selected to next generation with a larger probability. And the individuals cross and mutate to generate new individuals which represent new solutions. The latter generated populations will adapt to environment better than the previous populations. The individual which has the highest fitness value in last population after decoding is outputted as an optimal solution.

3.3.2 The Development of Stress Prediction Model GA-SVR. In order to use the advantages of GA, it was combined with SVR to construct the flow stress prediction model of Ti-6Al-4V alloy where GA was used to efficiently search the optimal parameter combination of the three parameters (C , γ , and ζ), i.e., the GA-SVR.

In this investigation, 2184 input-output pairs were selected from the experimental stress-strain curves, and 448 input-output pairs at the strain range of 0.05-0.8 with a distance of 0.05 were not used for training but for testing the generalization ability of the GA-SVR. The remaining 1736 input-output pairs were adopted to train the GA-SVR.

The N -fold cross-validation method, as an effective method for assessing the accuracy of data mining and machine learning, was adopted in this study to evaluate the performance of the GA-SVR. In N -fold cross-validation method, raw data are divided into N data sets. A separate dataset is retained as a validation dataset and the other ($N-1$) datasets are used to train the GA-SVR. Each dataset of N datasets is alternately set as validation dataset, and the performance of the GA-SVR is evaluated by the average number of an evaluation index in N validation process. In this work, the number N was set as 5. A classic evaluation index mean square error (MSE) between training stresses and validation stresses was introduced by Eq 6 to measure the fitness value.

$$MSE = \frac{1}{N} \sum_{i=1}^N [f(x_i) - y_i]^2, \quad (\text{Eq 6})$$

where $f(x_i)$ are the predicted stresses; y_i are the experimental stresses; and N is the number of stress-strain samples.

Besides, other representative evaluation index correlation coefficient (R) expressed as Eq 7 was adopted to assess the degree of correlation between the experimental flow stresses and predicted flow stresses (Ref 25). A larger R value indicates a well correlation between the two variables, and vice versa.

$$R = \frac{\sum_{i=1}^N (E_i - \bar{E})(P_i - \bar{P})}{\sqrt{\sum_{i=1}^N (E_i - \bar{E})^2 \sum_{i=1}^N (P_i - \bar{P})^2}}, \quad (\text{Eq 7})$$

where N is the number of samples; E is the sample of experimental stress-strain data; and P is the sample of predicted stress-strain data.

The detailed flowchart of the GA-SVR is shown in Fig. 3.

Step 1. Initialize the population of the GA-SVR. The parameters of the C , γ , and ζ were encoded to the chromosomes of individuals. In this work, the population number was set as 30.

Step 2. The fitness values of the individuals were computed by fitness function MSE expressed by Eq 6 in GA.

Step 3. The population was updated by the selection, crossover, and mutation operators. Based on the fitness value of

each individual, the individual which has a smaller *MSE* value was inherited to the next generation with a greater probability. Crossover probability P_C value is commonly set in the range of 0.6 to 0.9. A larger P_C value will fast bring new chromosomes to the population; nevertheless, it will increase the risk of premature convergence and the loss of well gene structure. While a smaller P_C value will delay the process of genetic evolution. In this study, the P_C value was set as 0.7. The mutation operator is used in local random searching, so the mutation probability P_m value should be set as a smaller value. In this work, P_m value was set as 0.01. The cross-validation method was adopted to evaluate the performance of the GA-SVR.

Step 4. Stop criterion. If the iteration times attains the predetermined times, the process of GA-SVR was stopped. Meanwhile the optimal parameters were outputted and further used to train the GA-SVR. In this work, the iteration times was set as 50.

Figure 4 exhibits the best fitness value and average fitness value corresponding to iteration times of the GA-SVR. As shown in Fig. 4, it can be seen that the convergence speed of the well-trained GA-SVR is fast. In the first 20 iteration times, the average fitness values sufficiently approximate to the best fitness value state. The C , γ , and ζ of the best parameter combination ($R = 0.99997$) are 99.95, 14.18, and 0.02, respectively.

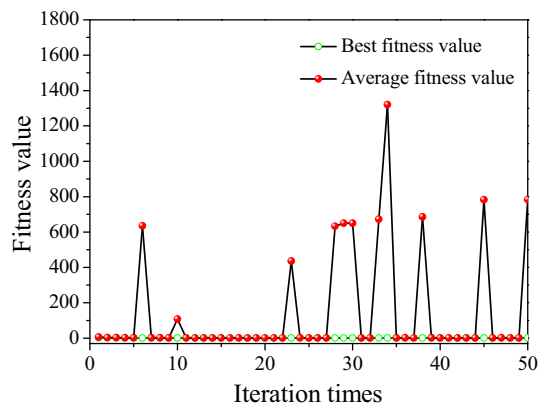


Fig. 4 The relationships between the fitness values and the iteration times of the GA-SVR

4. Comparisons of the Mathematical Regression Model, ANN, and GA-SVR for Ti-6Al-4V Alloy

In this chapter, the learning abilities, generalization abilities, and modeling efficiencies of the existing mathematical regression model, ANN, and GA-SVR for Ti-6Al-4V alloy were detailedly compared.

4.1 The Existing Mathematical Regression Model and ANN for Ti-6Al-4V Alloy

Quan et al. calculated the mathematical regression models at the strain of 0.5 for Ti-6Al-4V alloy in $(\alpha + \beta)$ phase and β phase by mathematical regression means, which just involve temperature and strain rate. The mathematical regression models in $(\alpha + \beta)$ phase and β phase were expressed as Eq 8 and 9, respectively (Ref 26).

$$\dot{\epsilon} = 1.43 \times 10^{25} [\sinh(0.0061\sigma)]^{4.70} \exp\left(\frac{-564.05}{RT}\right), \quad (\text{Eq 8})$$

$$\dot{\epsilon} = 1.94 \times 10^{11} [\sinh(0.0235\sigma)]^{3.36} \exp\left(\frac{-300.20}{RT}\right), \quad (\text{Eq 9})$$

where $\dot{\epsilon}$ is strain rate (s^{-1}); σ is flow stress (MPa); R is the universal gas constant (8.31 J/mol/K); and T is temperature (K).

And the ANN for Ti-6Al-4V alloy was described by Quan et al. in the reference (Ref 26).

4.2 Comparisons of the Study Abilities of the Mathematical Regression Model and GA-SVR

The classic evaluation index of relative error (δ) expressed as Eq 10 was adopted to estimate the performance of these prediction models

$$\delta(\%) = \frac{E_i - P_i}{E_i} \times 100\%, \quad (\text{Eq 10})$$

where E is the sample of experimental stress-strain values and P is the sample of predicted stress-strain values.

Other evaluation index of average absolute relative error (*AARE*) expressed by Eq 11 was adopted to further estimate the study abilities of these prediction models. Compared with δ value, *AARE* can better show total prediction error

Table 1 The singular points of testing predictions of GA-SVR

Temperature, K	Strain rate, s^{-1}	Strain	Experimental stress, MPa	Predicted stress, MPa, by GA-SVR	Relative error, %
1223	0.01	0.05	29.54131	30.96881	-4.8322
1223	0.01	0.8	26.00849	27.49151	-5.70206
1273	0.01	0.05	23.71685	25.42046	-7.18313
1273	0.01	0.8	21.49681	23.01901	-7.08107
1323	0.01	0.05	15.09013	17.02897	-12.8484
1323	0.01	0.8	16.15854	18.0067	-11.4377
1273	0.1	0.05	32.16834	33.92986	-5.47592
1273	0.1	0.8	35.76305	36.78041	-2.84474
1323	0.1	0.05	27.39279	28.72423	-4.86057
1323	0.1	0.8	34.1912	35.32371	-3.31228
1323	1	0.05	44.36162	45.90839	-3.48671
1323	10	0.05	61.08919	62.60452	-2.48052

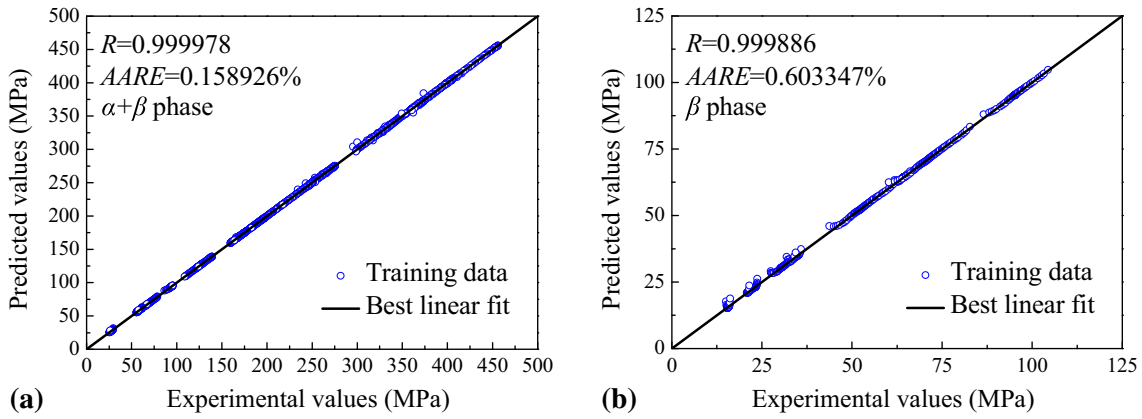


Fig. 5 Correlation between the trained flow stresses and training predictions for the training dataset of the GA-SVR model in ($\alpha + \beta$) phase and β phase

$$AARE = \frac{1}{N} \sum_{i=1}^N \left| \frac{E_i - P_i}{E_i} \right|, \quad (\text{Eq 11})$$

where E is the sample of experimental stress-strain values; P is the sample of predicted stress-strain values; and N is equal to the number of samples.

Figure 5 shows the correlation between the trained flow stresses and training predictions for the training dataset of the GA-SVR for Ti-6Al-4V alloy. As shown in Fig. 5, it can be observed that the R values between the trained flow stresses and training predictions of the GA-SVR model are larger than 0.999 at high accuracy levels. The R values of the mathematical regression models for Ti-6Al-4V alloy at the strain of 0.5 in ($\alpha + \beta$) phase and β phase are just 0.991 and 0.994, respectively (Ref 26). It can be summarized that the GA-SVR can sufficiently learn the training samples, and the study ability of the GA-SVR is stronger than the mathematical regression model. The mathematical regression model cannot precisely track the hot flow behaviors, because the multivariate nonlinear regression equation is difficult to describe the highly nonlinear flow behaviors which accompany phase transformation, WH, DRX, and DRV in wide temperature and strain rate ranges.

4.3 Comparisons of the Generalization Abilities Among the Mathematical Regression Model, ANN, and GA-SVR

Figure 6 shows the comparisons between the experimental flow stresses and testing flow stresses which were predicted by the GA-SVR at different strain rates and temperatures. The following work detailedly compared the generalization ability of the GA-SVR.

Figure 7 shows the correlation between the experimental flow stresses and testing flow stresses predicted by the GA-SVR in ($\alpha + \beta$) and β phase, and the R values between them are larger than 0.9998 at high accuracy levels. In order to detailedly display the distribution and relative frequency of δ values of the GA-SVR, they were further analyzed by Gaussian distribution analysis. The mean number of all the relative errors (μ) expressed as Eq 12 and standard deviation (w) expressed as Eq 13 were obtained after Gaussian distribution analysis. As expressed by Eq 13, the standard deviation (w) which is an evaluation index to measure discrete degree of individual in dataset was introduced to measure the distribution of the

relative error (δ). Here, a smaller w value demonstrates that most of δ values approach the μ value, and vice versa. And a smaller μ value indicates that more predicted stress data are close to the experimental stress data

$$\mu = \frac{1}{N} \sum_{i=1}^N \delta_i, \quad (\text{Eq 12})$$

$$w = \sqrt{\frac{1}{(N-1)} \sum_{i=1}^N (\delta_i - \mu)^2}, \quad (\text{Eq 13})$$

where δ is the sample of relative error; μ is the average number of δ values; and N is the number of samples.

As shown in Fig. 8, the δ values of the GA-SVR vary from -13 to 2% . Figure 8 shows the histogram of δ values of the GA-SVR, which show the relative frequency of each δ -level. The μ value and w value of the GA-SVR are 0.00702 and 0.52684. It can be observed that most of δ values (97.322%) distribute in the range of -2 to 2% , and few δ values (2.678%) are smaller than -2% . The few δ values (2.678%) which are smaller than -2% are some singular points of the testing predictions, and they also can be seen from Fig. 6 and 7. And these singular points are shown in Table 1. It can be observed that these singular points locate the edge of the stress-strain curves. Some data points which locate the edge of the stress-strain curves and do not accord with the whole tendency of the hot flow behaviors are more likely to be appropriately ignored. It should be noted that some singular points cannot influence the accuracy of the entire model. The testing predictions in Table 1 are close to the experimental stresses, which do not influence the accuracy of the entire model.

Peng et al. established an ANN for the flow behaviors of as-cast Ti60 titanium alloy during hot deformation, and the correlation coefficient (R) in their work is 0.992 (Ref 17). Zhu et al. predicted flow stress in isothermal compression of as-cast TC21 titanium alloy, and the correlation coefficient (R) in their work is 0.992 (Ref 18). Table 2 exhibits the R values and $AARE$ values of testing dataset of the ANN and GA-SVR, so as to further compare the generalization abilities of them. It can be observed that the GA-SVR has larger R values and lower $AARE$ values, which indicate that the GA-SVR can accurately predict the highly nonlinear flow behaviors. Compared with ANN, the

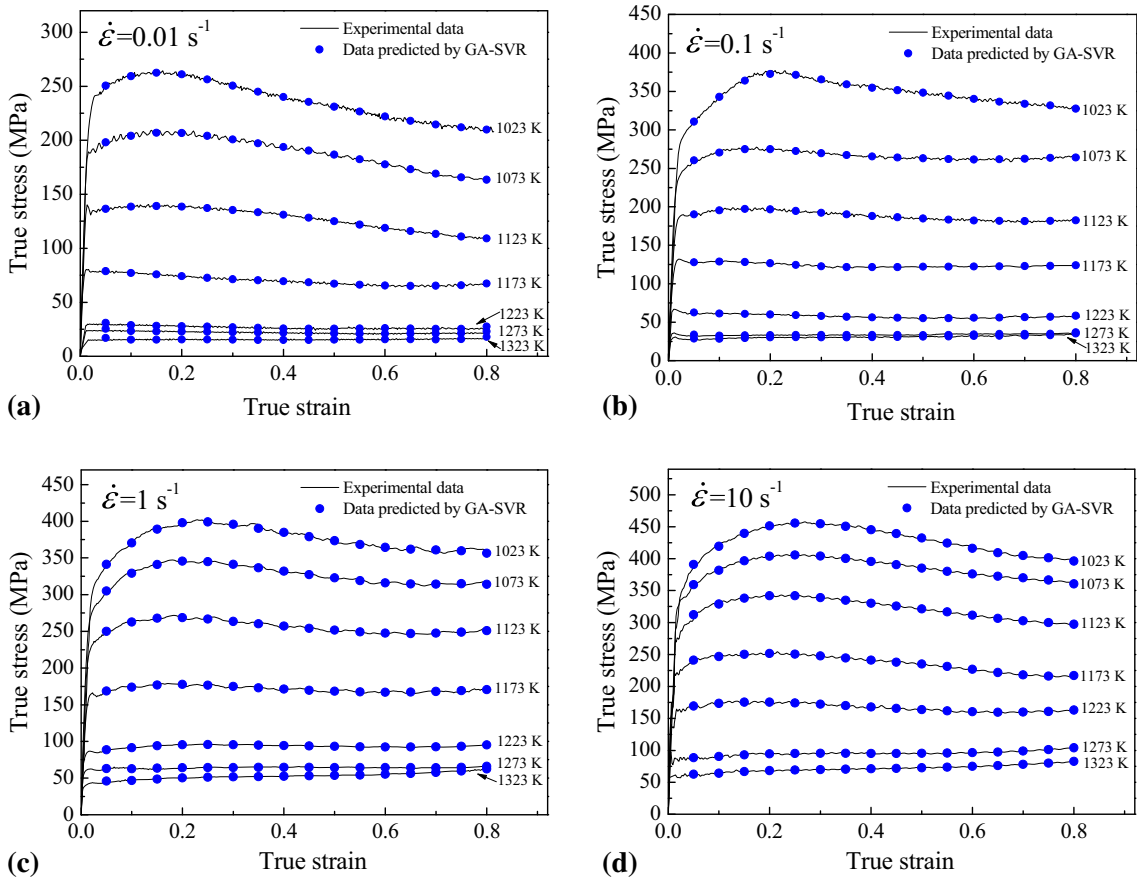


Fig. 6 Comparisons between the experimental flow stresses and the testing flow stresses predicted by the GA-SVR at different strain rates and temperatures

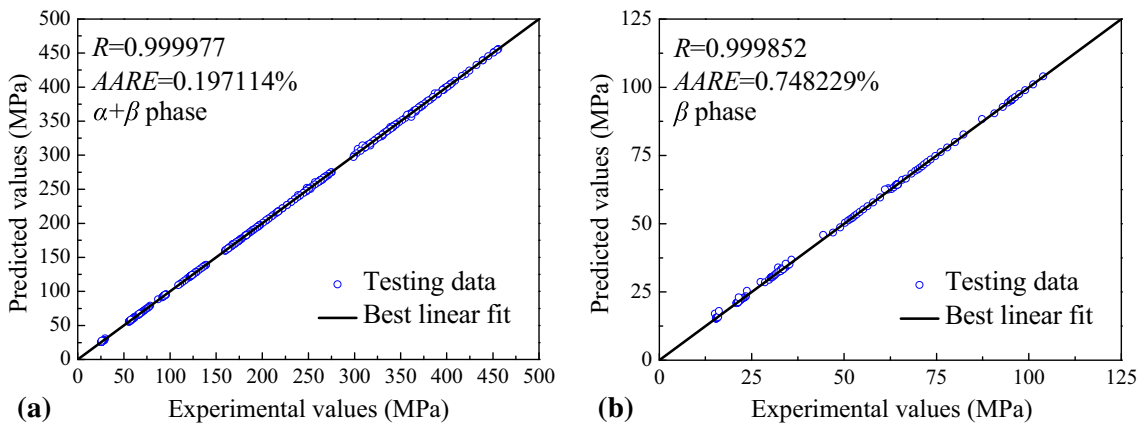


Fig. 7 Correlation between the experimental flow stresses and the testing flow stresses predicted by the GA-SVR in $(\alpha + \beta)$ and β phase

globally optimal solution can be obtained using GA-SVR, and the computational processes of GA-SVR are robust and will avoid falling into local extreme value. For a certain dataset, the same network topology and training parameters of an ANN will attain fluctuant accuracies in different attempts. ANN can encounter well network topology and training parameters to reach a higher accuracy level; however, this accurate results have poor reproducibility. The significant character of SVR is

that a SVR with same training parameters can keep training accuracy and prediction accuracy at a stable level in different attempts for a certain dataset. The generalization ability of GA-SVR is stronger than ANN. The mathematical regression model cannot precisely study the hot flow behaviors, and its generalization ability is poor. The generalization abilities of these models were displayed as follows in ascending order: the mathematical regression model < ANN < GA-SVR.

Table 2 The *R* values and *AARE* values between the experimental flow stresses and predicted flow stresses of the ANN and GA-SVR for Ti-6Al-4V alloy

Model	<i>R</i> value		<i>AARE</i> value	
	ANN	GA-SVR	ANN	GA-SVR
($\alpha + \beta$) phase	0.9999	0.999977	0.51%	0.197114%
β phase	0.9998	0.999851	0.79%	0.7482294%

Table 3 The time in modeling an accurate model of the mathematical regression model, ANN, and GA-SVR

Model	Mathematical regression model	ANN	GA-SVR
The time in modeling an accurate model	More than 180 min	More than 60 min	About 15 min

4.4 Comparisons of the Modeling Efficiencies Among the Mathematical Regression Model, ANN, and GA-SVR

Table 3 exhibits the time in constructing an accurate model of the mathematical regression model, ANN, and GA-SVR. Mathematical regression model needs to calculate numerous material constants and construct many multivariate nonlinear regression equations based on limited experimental data. And these material constants and regression models need to be recomputed when some new stress data are involved. This process is complex and time-consuming. GA-SVR does not need to calculate material constants and complicated mathematical regression equations. GA-SVR only needs representative training samples from the investigation and then automatically searches the three parameters *C*, γ , and ζ to obtain the most accurate model.

ANN needs to try a lot of network topologies and training parameters to acquire a higher accuracy level, which consumes much time and energy. Besides, the training process of ANN is instable. For a certain dataset, the same network topology and training parameters of an ANN will obtain fluctuant accuracies in different attempts, which decreases the modeling efficiency. Based on the selection, crossover, and mutation operators, GA-SVR can self-adaptively and dynamically search the optimal parameters, which greatly enhances the computational efficiency. And the computing time of a training process of SVR is shorter than ANN. The modeling efficiencies of these models were displayed as follows in ascending order: the mathematical regression model < ANN < GA-SVR.

5. Applications of the GA-SVR in Forming Simulation

The flow stress data at the strain rate of 10 s^{-1} and temperatures of 1048, 1098, 1148, 1198, 1248, and 1298 K were predicted for Ti-6Al-4V alloy by the GA-SVR. And the predicted stress-strain curves at the strain rate of 10 s^{-1} and temperatures of 1023-1323 K are shown in Fig. 9. The expanded stress-strain curves are beneficial to accuracy improvement in following fields.

In this chapter, the impact of input stress-strain curves on simulation results of compression test was analyzed by a FEM software DEFORM. The simulation parameters were set based on the actual compression experiments. One half of the test sample was simulated for the reason of geometric symmetry, so

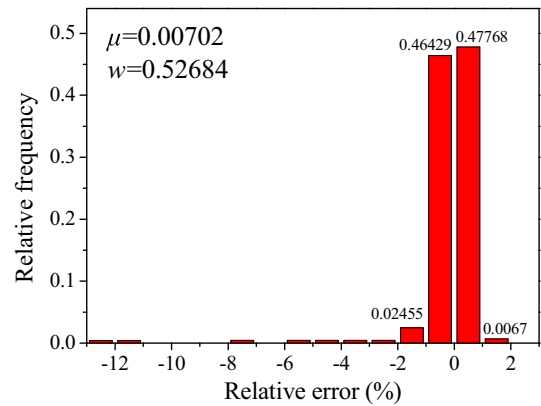


Fig. 8 Distributions of relative errors of testing data of GA-SVR

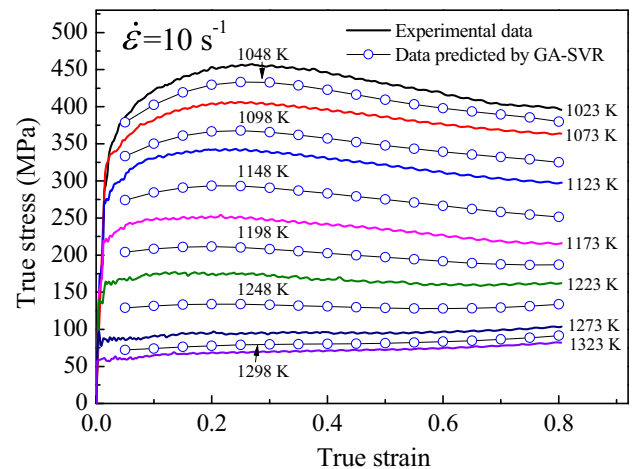


Fig. 9 The true stress-strain curves of Ti-6Al-4V alloy at the strain rate of 10 s^{-1} and temperatures of 1023-1323 K, in which the solid curves are experimental data and the fitted curves by points are predicted data

as to decrease the computing time. In the actual compression experiments, the top and bottom surfaces of the test sample were coated with graphite lubricants to diminish friction between the sample and anvils, thereby, the friction type among the contact surfaces of the sample and dies was set as

shear-type in DEFORM. The heat conduction and heat radiation among test sample, dies, and ambient were neglected to simulate the isothermal compression test. If finite element software needs to invoke stress-strain data which are not beforehand inputted to the software, it commonly calculates unknown stress-strain data by mathematical interpolation means. However, hot flow behaviors of materials at different strain rates and temperatures are highly nonlinear. The mathematical interpolation way cannot correctly predict the stress-strain data of materials and will obtain incorrect simulation results. Therefore, in this chapter, the expanded stress-strain curves predicted by GA-SVR were applied to enrich the stress data of Ti-6Al-4V alloy.

Two simulation schemes were designed for analyzing the influences of input stress-strain curves on final simulation results. The whole initial conditions of the two simulation schemes are same except for different input stress-strain curves. The compression tests were simulated at the strain rate of 10 s^{-1} and temperature of 1123 K. The stress-strain curves at strain rate of 10 s^{-1} and temperatures of 1023-1323 K which contain the expanded data were applied to scheme-A. The experimental stress-strain curves at the temperatures of 1023, 1073, 1173, 1223, 1273, and 1323 K and strain rate of 10 s^{-1} were adopted by scheme-B, so the stress-strain curve at the

temperature of 1123 K and strain rate of 10 s^{-1} needs to be automatically interpolated by software.

Figure 10(a) and (b) displays the distributions of effective stresses of scheme-A and scheme-B, which can be approxi-

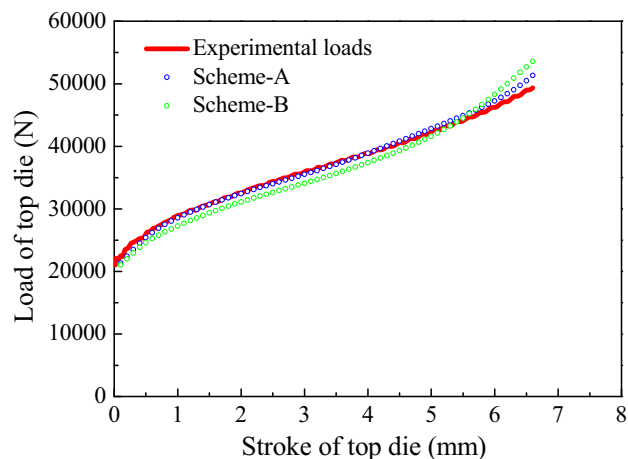


Fig. 11 The relationship between the stroke and the load of top die of experimental data, scheme-A, and scheme-B

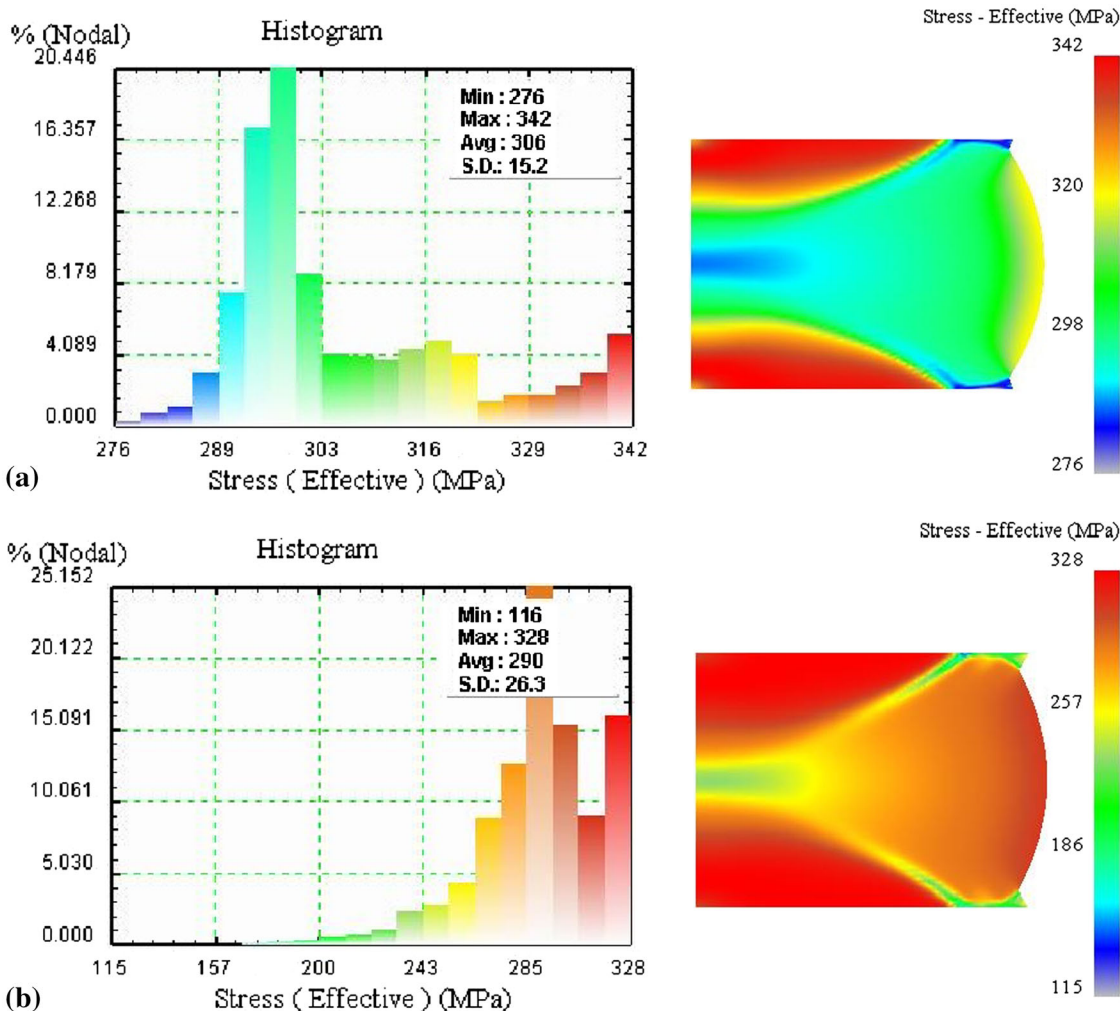


Fig. 10 Distributions of effective stress for (a) scheme-A (b) scheme-B at the strain rate of 10 s^{-1} , temperature of 1123 K, and strain of 0.8

mately divided into three districts. However, there exist large differences of distributions of effective stresses between scheme-B and scheme-A, as well as the average effective stress.

In addition, as shown in Fig. 11, the load curves of top dies of scheme-A and experimental values are very close. The relative errors of the top die loads between scheme-A and experimental values are in the range of -3.767153 to 4.134918% , whereas this errors between scheme-B and experimental values are in the range of -8.293616 to 6.218511% . It can be summarized that a large span of interpolation or insufficient stress-strain data bring inaccurate simulation results. In addition, hot flow behaviors under different strain rates and temperatures of a material are highly nonlinear, thereby, calculating stress data by interpolation way in FEM software is inaccurate. It is universally acknowledged that stress-strain data play important roles in many fields, for examples, speculating WH and DRV (Ref 1), improving processing maps (Ref 2), characterizing dynamic recrystallization evolution (Ref 3), etc. The GA-SVR can accurately predict flow behaviors of materials, which can improve the related research fields where stress-strain data play important roles.

6. Conclusions

The novel prediction model GA-SVR was constructed for characterizing the hot flow behaviors of Ti-6Al-4V alloy according to the experimental stress-strain data. Following conclusions were concluded from the current investigation:

- (1) The R values and $AARE$ values between trained flow stresses and training predictions for the training dataset of the GA-SVR in $(\alpha + \beta)$ phase and β phase are 0.999978 and 0.158926 and 0.999886 and 0.603347%, respectively. The results indicate the GA-SVR model can sufficiently study the hot flow behaviors which accompany with WH, DRX, and DRV. Comparison results show that the learning ability of the GA-SVR is stronger than the mathematical regression model.
- (2) In the comparisons of generalization abilities of these models, the R values and $AARE$ values between the experimental flow stresses and testing flow stresses which were predicted by the GA-SVR in $(\alpha + \beta)$ and β phase are 0.999977 and 0.197114 and 0.999852 and 0.748229%, respectively. The results indicate the GA-SVR can precisely predict the highly nonlinear flow behaviors of Ti-6Al-4V alloy. The generalization abilities of these models were shown as follows in ascending order: the mathematical regression model < ANN < GA-SVR.
- (3) According to the selection, crossover, and mutation operators, the GA-SVR can self-adaptively and dynamically search the optimal parameter combination of the three parameters (C , γ , and ζ), which greatly improves the computational efficiency. The modeling efficiencies of these models were shown as follows in ascending order: the mathematical regression model < ANN < GA-SVR.
- (4) Hot flow behaviors of materials at different strain rates and temperatures are highly nonlinear. In finite element software, the mathematical interpolation way cannot correctly predict the stress-strain data of materials and will obtain incorrect simulation results. The stresses outside experimental conditions were predicted by the well-

trained GA-SVR, which improved simulation accuracy of the load-stroke curve and can further improve the related research fields where stress-strain data play important roles.

Acknowledgments

The project was supported by Beijing Finance Found of Young Prominent Talent Project (No. 2014000026833ZK25) and Young Talents Project (No. 2014000020124G096).

References

1. L. Li, B. Ye, S. Liu et al., Inverse Analysis of the Stress-Strain Curve to Determine the Materials Models of Work Hardening and Dynamic Recovery, *Mater. Sci. Eng. A*, 2015, **636**, p 243–248
2. G.-Z. Quan, Y. Wang, C.-T. Yu et al., Hot Workability Characteristics of As-Cast Titanium Alloy Ti-6Al-2Zr-1Mo-1V: A Study Using Processing Map, *Mater. Sci. Eng. A*, 2013, **564**, p 46–56
3. G.-Z. Quan, G.-S. Li, T. Chen et al., Dynamic Recrystallization Kinetics of 42CrMo Steel During Compression at Different Temperatures and Strain Rates, *Mater. Sci. Eng. A*, 2011, **528**(13–14), p 4643–4651
4. Y.C. Lin, Q.-F. Li, Y.-C. Xia et al., A Phenomenological Constitutive Model for High Temperature Flow Stress Prediction of Al-Cu-Mg alloy, *Mater. Sci. Eng. A*, 2012, **534**(1), p 654–662
5. H.-Y. Li, J.-D. Hu, D.-D. Wei et al., Artificial Neural Network and Constitutive Equations to Predict the Hot Deformation Behavior of Modified 2.25Cr-1Mo Steel, *Mater. Des.*, 2012, **42**, p 192–197
6. G.-Z. Quan, W.-Q. Lv, Y.-P. Mao et al., Prediction of Flow Stress in a Wide Temperature Range Involving Phase Transformation for As-Cast Ti-6Al-2Zr-1Mo-1V Alloy by Artificial Neural Network, *Mater. Des.*, 2013, **50**(17), p 51–61
7. X.G. Fan, H. Yang, and P.F. Gao, Prediction of Constitutive Behavior and Microstructure Evolution in Hot Deformation of TA15 Titanium Alloy, *Mater. Des.*, 2013, **51**, p 34–42
8. G.Z. Voyiadjis and F.H. Abed, Microstructural Based Models for bcc and fcc Metals with Temperature and Strain Rate Dependency, *Mech. Mater.*, 2005, **37**(2–3), p 355–378
9. S.V. Sajadifar and G.G. Yapici, Workability Characteristics and Mechanical Behavior Modeling of Severely Deformed Pure Titanium at High Temperatures, *Mater. Des.*, 2014, **53**(1), p 749–757
10. J. Xiao, D.S. Li, X.Q. Li et al., Constitutive Modeling and Microstructure Change of Ti-6Al-4V During the Hot Tensile Deformation, *J. Alloys Compd.*, 2012, **541**(1), p 346–352
11. A.S. Khan, R. Kazmi, B. Farrokh et al., Effect of Oxygen Content and Microstructure on the Thermo-mechanical Response of Three Ti-6Al-4V Alloys: Experiments and Modeling over a Wide Range of Strain-Rates and Temperatures, *Int. J. Plast.*, 2007, **23**(7), p 1105–1125
12. A.S. Khan, Y. Sung Suh, and R. Kazmi, Quasi-static and Dynamic Loading Responses and Constitutive Modeling of Titanium Alloys, *Int. J. Plast.*, 2004, **20**(12), p 2233–2248
13. N. Kotkunde, A.D. Deole, A.K. Gupta et al., Comparative Study of Constitutive Modeling for Ti-6Al-4V Alloy at Low Strain Rates and Elevated Temperatures, *Mater. Des.*, 2014, **55**(6), p 999–1005
14. Z. Akbari, H. Mirzadeh, and J.-M. Cabrera, A Simple Constitutive Model for Predicting Flow Stress of Medium Carbon Microalloyed Steel During Hot Deformation, *Mater. Des.*, 2015, **77**, p 126–131
15. J. Liu, W. Zeng, Y. Lai et al., Constitutive Model of Ti17 Titanium Alloy with Lamellar-Type Initial Microstructure During Hot Deformation Based on Orthogonal Analysis, *Mater. Sci. Eng. A*, 2014, **597**, p 387–394
16. Y.C. Lin, G. Liu, M.-S. Chen et al., Prediction of Static Recrystallization in a Multi-pass Hot Deformed Low-Alloy Steel Using Artificial Neural Network, *J. Mater. Process. Technol.*, 2009, **209**(9), p 4611–4616
17. W. Peng, W. Zeng, Q. Wang et al., Comparative Study on Constitutive Relationship of As-Cast Ti60 Titanium Alloy During Hot Deformation

- Based on Arrhenius-Type and Artificial Neural Network Models, *Mater. Des.*, 2013, **51**(5), p 95–104
18. Y. Zhu, W. Zeng, Y. Sun et al., Artificial Neural Network Approach to Predict the Flow Stress in the Isothermal Compression of As-Cast TC21 Titanium Alloy, *Comput. Mater. Sci.*, 2011, **50**(5), p 1785–1790
 19. H. Wang, E. Li, and G.Y. Li, The Least Square Support Vector Regression Coupled with Parallel Sampling Scheme Metamodeling Technique and Application in Sheet Forming Optimization, *Mater. Des.*, 2009, **30**(5), p 1468–1479
 20. Y. Lou, C. Ke, and L. Li, Accurately Predicting High Temperature Flow Stress of AZ80 Magnesium Alloy with Particle Swarm Optimization-based Support Vector Regression, *Appl. Math. Inf. Sci.*, 2013, **7**(3), p 1093–1102
 21. R.K. Desu, S.C. Guntuku, B. Aditya et al., Support Vector Regression Based Flow Stress Prediction in Austenitic Stainless Steel 304, *Procedia Mater. Sci.*, 2014, **6**, p 368–375
 22. R. Sivaraj and T. Ravich, An Improved Clustering Based Genetic Algorithm for Solving Complex NP Problems, *J. Comput. Sci.*, 2011, **7**(7), p 1033–1037
 23. T. Sakai, A. Belyakov, R. Kaibyshev et al., Dynamic and Post-dynamic Recrystallization Under Hot, Cold and Severe Plastic Deformation Conditions, *Prog. Mater. Sci.*, 2014, **60**(1), p 130–207
 24. S.S. Keerthi and C.-J. Lin, Asymptotic Behaviors of Support Vector Machines with Gaussian Kernel, *Neural Comput.*, 2003, **15**(7), p 1667–1689
 25. R.-X. Chai, C. Guo, and L. Yu, Two Flowing Stress Models for Hot Deformation of XC45 Steel at High Temperature, *Mater. Sci. Eng. A*, 2012, **534**, p 101–110
 26. G.-Z. Quan, H.-R. Wen, P. Jia et al., Construction of Processing Maps Based on Expanded Data by BP-ANN and Identification of Optimal Deforming Parameters for Ti-6Al-4V Alloy, *Int. J. Precis. Eng. Manuf.*, 2016, **17**(2), p 171–180